Luminescence dosimetry for evaluation of the external exposure in Metlino, upper Techa River valley, due to the shore of the Metlinsky Pond: a feasibility study

Woda, C.[1,*] , Hiller, M.[2], Ulanowski, A.[1,3], Bugrov, N.G.[4], Degteva, M.O.[4], Ivanov, O[5], Romanov, S[6], Tschiersch, J.[1], Shinonaga, T.[7,†]

[1] *Helmholtz Zentrum München, Institute of Radiation Medicine, 85764 Neuherberg, Germany*

[2]*Independent Researcher, Stolberg, Germany*

[3]*International Atomic Energy Agency, IAEA Environmental Laboratories, A-2444 Seibesdorf, Austria*

[4] *Urals Research Center for Radiation Medicine, Chelyabinsk, Russia*

[5] *National Research Center «Kurchatov Institute», Moscow, 123182, Russia*

[6]*Southern Urals Biophysics Institute, Ozyorsk, Russia*

[7]*Helmholtz Zentrum München, former Institute of Radiation Protection, 85764 Neuherberg, Germany*

Abstract

Luminescence dosimetry was performed using bricks from the former settlement of Metlino, Southern Urals, Russia, to investigate the feasibility of validating the Techa River Dosimetry System (TRDS) 2016 for the shore of the Metlinsky Pond, upper Techa River region. TRDS is a code for estimating external and internal doses for members of the Extended Techa River Cohort. Several brick samples were taken from the north-western wall of the granary, facing the Metlinsky Pond. Samples were measured at different heights and at different depths into the bricks. Dating of the granary was performed by analyzing well shielded bricks. Assessment of the gamma dose-rate at the sample positions was done by thermoluminescent dosimeters and the dose-rate in front of the granary mapped with a dose-rate meter. Anthropogenic doses in bricks vary from 0.8 to 1.7 Gy and show an increase with sampling height. A similar height profile is observed for the current gamma dose-rate, which is compatible with the results of the dose-rate mapping. Implications for validating the TRDS are discussed.

Keywords: Luminescence, OSL, TL, dose reconstruction, quartz, TRDS, Southern Urals Radiation Risk Research

[*] Corresponding author. Tel.: +49 89 3187 2802, fax: +49 89 3187 3363, Email: clemens.woda@helmholtz-muenchen.de

[†] present address: Hirosaki University, Institute of Radiation Emergency Medicine, Aomori 036-8564, Japan

1. Introduction

Previous studies have shown that luminescence techniques, in combination with Monte Carlo calculations, can be successfully applied for using ceramic building materials, such as bricks and tiles, to determine the external gamma dose in radioactively contaminated settlements (Bailiff et al., 2004a; Bailiff et al., 2004b; Goksu and Bailiff, 2006; Hiller et al., 2017; Jacob et al., 2003; Meckbach et al., 1996; Taranenko et al., 2003; Woda et al., 2011a). In this work, measurement results are presented which can be used to validate the integral air kerma value at the Techa River banks, Southern Urals, Russia. This air kerma value is a key input parameter of the Techa River Dosimetry System (TRDS-2016), a code which is used to calculate estimates of the external and internal doses for the exposed population of the villages along the Techa River (approximately 30000 people). Radioactive contamination of the Techa River occurred in 1949–1956 due to discharges of liquid radioactive waste by the Mayak plutonium facility. The focus of the present study is the former village of Metlino, located 7 km downstream of the release point, where the highest doses of external exposure of the inhabitants occurred. Considerable effort has been undertaken earlier to support dose reconstruction for the TRDS-2016 using reference points at the Techa River shoreline at Metlino (Degteva et al 2008). However, a similar validation study for the air kerma in reference points at the shore of the Metlinsky Pond, also used in TRDS-2016, has not yet been carried out. According to Degteva et al. (2008), the Metlinsky Pond could be the major source of external exposure of the Metlino population. The existing remains of brick buildings on the site of the former village, like the remaining north-western wall of the former granary facing the Metlinsky Pond, allow for a validation study by using the brick samples as a dose archive. A particular challenge for such dose reconstruction in this site comes from the fact that after relocation of the residents in 1956 and demolition of most of the houses a new reservoir lake was created. In this way the contaminated banks and floodplains were covered with and shielded by water, which considerably changed the exposure geometry for the remaining brick buildings (mill, granary, church).

In this work, brick samples from the north-western wall of the granary were measured to assess the dose in brick due to anthropogenic sources. In addition, the external gamma dose-rates at the brick sample positions were monitored and the dose-rate above soil was mapped for a larger area in front of the granary. The results presented in this paper provide an independent experimental basis for a full-scale validation study of the TRDS-2016. In the latter, results of the luminescence measurements in combination with photon transport calculations will be used to assess anthropogenic doses in air at the shore of the Metlinsky Pond.

2. Material and methods

2.1 The sample site and sample collection

Fig. 1**Error! Reference source not found.** illustrates the evolution of the sampling site from the time when the village was intact and populated to today. Most of the original houses and buildings were destroyed when the settlement was evacuated in 1956, only the parts of the old mill, granary and the church remain today. All are located close to the former Techa River banks and floodplains, the mill and granary also close to the Metlinsky pond shoreline.

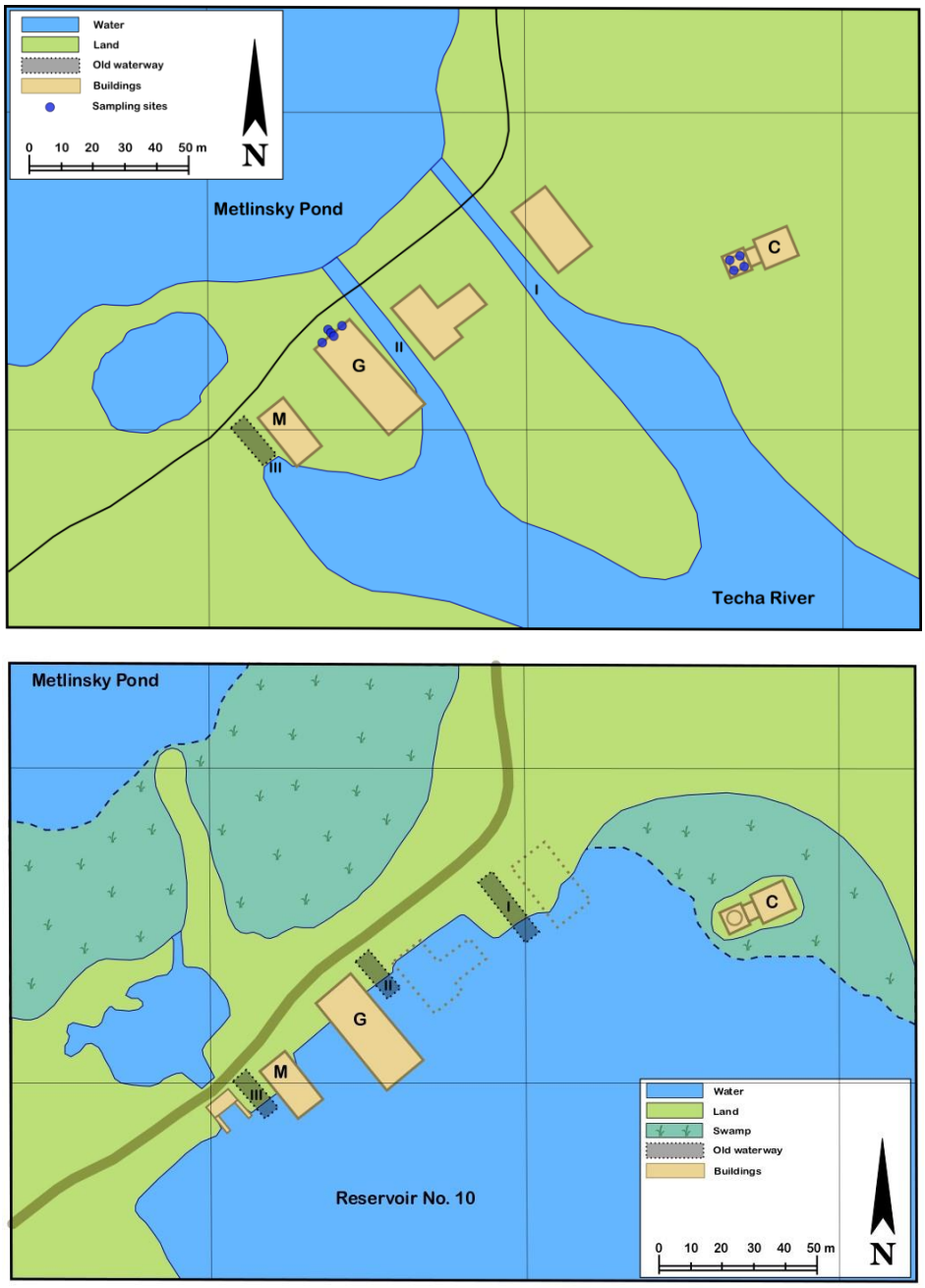

Fig. 1. Upper panel: Map (Sketch) of the hydrological system at Metlino, including the main buildings mill (M), granary (G) and church (C), as revealed by the declassification of historical documents (Mokrov et al. 2005), for the time period of 1949-1956, when the village was intact. The waterways are indicated by Roman numerals. Lower panel: Sketch of the sampling site as it is today. Through the creation of Reservoir No. 10, parts of the former village and the Techa riverbed, contaminated banks and floodplain are covered with water. In addition, sediments have accumulated in the former shoreline area of the Metlinsky pond northwest of the granary, creating a swampy area. The former, now no longer operative, waterways are indicated by grey shaded areas.

From the north-western wall of the granary, facing the Metlinsky pond, seven locations for brick sampling were chosen in a field trip in June 2007 and a total of nine samples were extracted, labelled G1 to G9 (Fig. 2). Samples were taken from three different heights, which helps constrain the possible source configurations. Bricks were chosen, which were located as much as possible in uniform brickwork at sufficient distance from windows, doors and obstructing elements. Samples G1/2, G3 and G4 were taken from the same spot, to analyse the degree of variability in dose measurements, whereas samples G5 and G6 were taken from the same height but separated by several meters to assess the horizontal homogeneity of dose deposition along the granary wall. Analysis in the laboratory revealed that no dose could be measured for sample G9 due to very little amount of extractable quartz grains and insufficient signal to noise ratio of the luminescence signal from these grains. Therefore four new samples, G10-14 were collected in 2009 in adjacent positions around G9. Generally, intact bricks or brick pieces of sufficient length could be extracted for all sampling positions, enabling the measurement of a dose-depth profile for verification of source energy. Heights of the sampling points in Tables 2-4 are given above the water level in the Reservoir No. 10. At all sample positions, the dose-rate was measured with a hand-held dose-rate meter (Automess 6150 AD 6/E). At selected sample positions, holes were drilled in three adjacent bricks around the sample, and Thermoluminescence dosimeters (TLDs), made of Al_2O_3:C and put in casings of copper, deposited within. The TLDS were fixed with glue, to avoid removal by birds. The dosimeters were retrieved after one year, read out and calibrated.

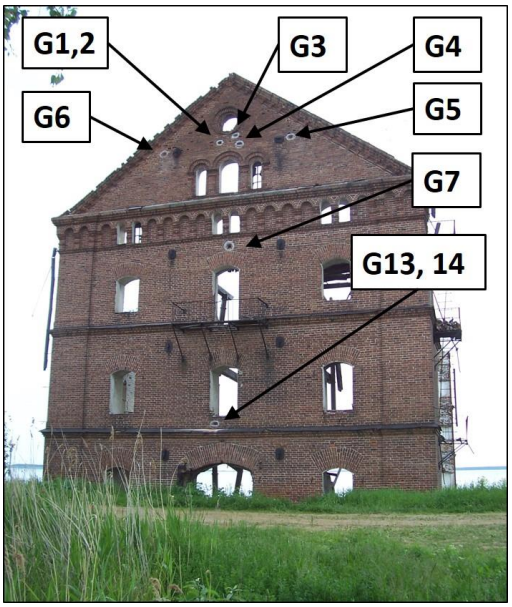

Fig.1. Sample positions on the NW wall of the granary .

For assessing the background dose (see below), two bricks from shielded locations were sampled, one from the first floor near a corner (BG-G-1), the second from a bricked window in the

same floor (BG-G3). From both bricks, a smaller piece from the back, facing the wall, was cut for preparation and analysis. These brick parts were shielded by > 30 cm of bricks to the left, right, back (facing the Metlinsky Pond) and front (facing the Reservoir 10), for sample BG-G-1 also by ~ 14 cm bricks to the top. For both samples, three to five depth intervals were cut, prepared and measured separately to check for sufficient shielding from the contaminated sources.

2.2 Field measurements

Field measurements were performed at four field trips in the years 2007, 2008, 2011 and 2012. At each field trip, dose rate measurements in air were performed using the dose rate meter described above. Measurements were performed at height 1 m above ground. The goal of the measurements was to map the dose rate in the area in front of the Granary towards the Metlinsky Pond. As reference point, measurements started on the road in front of the granary (shown in grey in Figure 1, bottom panel). Measurements were performed on straight lines perpendicular to the road towards the Metlinsky Pond, as far as the water line would allow. The distance between measurement points was no longer than 5 m, often shorter when needed to reflect the shape of the terrain. In dry years, the water level in the Metlinsky Pond was reduced, exposing a few more meters of shoreline, making it accessible for measurements. In those years, measured dose rates were usually higher, due to the lack of shielding from the water in the Metlinsky Pond. This was especially the case for the swamp in front of Granary, where the languet stretches out towards the Metlinsky Pond. Performing the measurements in several years allowed to compensate for environmental factors linked to precipitation and water levels in the area, as averages over all measurements taken at the same spot can be calculated.

At seven locations additional TLDs were fixed to wooden sticks and positioned 1 m above ground on 19 September 2012. Two TLDs per location were in casings of copper, two in casings of aluminium. TLDs were retrieved on 4 December 2012 and sent to HMGU for analysis in January 2013.

2.3 Sample preparation

Brick samples were prepared in the laboratory under subdued red light conditions. The first five millimetres of the exposed surface were removed to avoid bleached material. Two depth intervals were then cut for each brick at 1 and either 2 or 3 cm depth (thickness of 0.5 or 1 cm each) as measured from the brick surface. For samples G1/2, G7 and G14, additional depth intervals up to a depth of 8 cm were cut for measurement of a dose-depth profile. Quartz in the grain size fraction of 140–200 µm was then extracted using standard separation techniques, including treatment with HCl for 1 h in an ultrasonic bath and 40% HF for 40-60 min, followed by an additional HCl treatment and subsequent wet sieving (Aitken, 1985).

2.2 Luminescence measurements

2.2.1 TLDs

Before deposition, the TL dosimeters were annealed in a muffle furnace in air at 900°C for 1 hour. After retrieval, the TLDs were then measured in a Risø TL-DA-10 automated reader, without a built-in beta source to avoid scattered radiation, up to 400°C at a heating rate of 2°C s^{-1}. The integral of the glow curve from 100 -250°C was used for intensity determination. To convert the signal intensity into absorbed dose, the TLDs were subsequently irradiated with a ^{137}Cs source of the Secondary Standard Dosimetry Laboratory at HMGU,using 2 mm PMMA in front of the TLDs as a built-up layer, and then measured again. Calibration doses were 10-20 mGy for the dosimeters stored in the granary wall and 50 mGy for the dosimeters placed above soil. The dose accumulated in the TLDs during transport from the laboratory in Munich to and from the sampling site was determined in a previous field trip to Muslyumovo using separate transport dosimeters as 40±10 µGy. For calculating the background dose in the TLDs, both for the time periods of storage in the granary wall and above soil and for the time period in the lab prior to measurement, an average background dose rate of (0.7±0.2) mGy a^{-1} was used. This value was calculated from the average specific activities of naturally occurring radionuclides in bricks from the sampling site, from the assumed specific activities in soil and using the conversion factors reported in Ulanowski et al. (2019). Furthermore, for the TLDs placed above soil, of the 76 days of storage, 21 days were with an average snow cover of 10 cm (information retrieved from the online weather archive for Chelyabinsk at rp5.ru). From radiation transport calculations using the Monte Carlo Code MCNP6.2 (Werner et al., 2017), the reduction of radiation from ^{137}Cs distributed homogeneously in soil up to a depth of 30 cm by a 10 cm snow cover was calculated as 15%. Using the same transport code and radionuclide distribution, the ratio of dose in air to dose in TLD 1m above ground was calculated as 1.0 for the casing made of copper and 0.96 for the casing made of aluminium. The various factors were used to convert the dose measured in TLDs to an average dose-rate in air above soil without snow cover, for comparison with the results of the dose-rate measurements using the Automess device. For the TLDs at 1 cm depth in the brick wall, the ratio of dose in TLD to dose in brick (quartz grains) ranges from 0.62-0.65, depending on height (Ulanowski et al., 2019).

2.2.1 Quartz from bricks

OSL measurements were performed on a Risø TL/OSL-DA-15 automated reader, equipped with blue LEDs (470±30 nm) for stimulation and a Thorn-EMI 9235 photomultiplier combined with a 7.5 mm U-340 Hoya filter (290–370 nm) for detection. TL measurements were performed on a Risø TL-DA-12 automated reader, equipped with the same photomultiplier tube but using a a heat-absorbing filter HA-3 together with a blue (300–500 nm) transmitting BG12 glass filter for detection. Each sample was divided into 18-21 aliquots, with usually six aliquots used for TL and 12-15 for OSL. For OSL the cumulative dose D_L was measured using a single aliquot regenerative

dose (SAR) protocol with test dose normalisation (Murray and Wintle, 2003). The OSL curve was recorded for 40 s at 125°C. A preheat temperature of 190°C was chosen and a cutheat temperature for measuring the OSL response to the test dose was set to 160°C. The choice of parameters is based on experiences with bricks form another settlement in the same area (Woda et al., 2011b). Comparative measurements on selected samples using different preheat temperatures ranging from 190°C to 280°C, in some cases also applying an additional OSL readout at high temperature (280°C) at the end of the test dose measurement sequence (so called "hot bleach", Wintle and Murray (2006)), yielded statistically indistinguishable results for the absorbed dose . TL measurements of the cumulative dose D_L was only performed for those samples where the restricted Single Aliquot Regeneration (SAR) protocol using the 210°C TL peak was applicable. In this protocol, recording of the glow curve is terminated at 270°C at a heating rate of 3°C/s (Bailiff et al., 2000; Bailiff and Petrov, 1999), which generally avoids significant sensitivity changes. A preheat of 100 s at 160°C was applied (Woda et al., 2011b), which yielded extended dose plateaus as a function of recorded temperature for most samples. The temperature interval over which the TL signal was integrated was chosen individually for each aliquot, based on the dose plateau but generally was between 180°C and 230°C.

For OSL the error of a measurement was calculated using the approach described in Galbraith (2002), for TL considering counting statistics and fluctuations in the dark current of the PM tube. The error of the interpolated cumulative dose D_L for one aliquot was then assessed by propagated errors of the parameters of the weighted linear fit. From the set of aliquots, which were measured per sample, the weighted mean of the dose values of the aliquots was calculated along with the internal and external error variances σ_{in}^2 and σ_{ext}^2 (see Woda et al. (2011 a) for further details). For the statistical variance of the cumulative dose of a sample, the larger of the two values σ_{in}^2 and σ_{out}^2 was used. The variance of the cumulative dose was then calculated as the sum of the statistical variance and of the variance of the calibration of the beta source (error of 3.5 %). It is assumed that the uncertainty in the beta source calibration is normally distributed.

2.3 Determination of background dose

To assess the absorbed dose due to anthropogenic sources in the bricks (D_X) the background dose (D_{BG}) due to natural sources of radiation must be subtracted from the cumulative absorbed dose (D_L), measured with TL or OSL. This can be expressed as:

$$D_X = D_L - D_{BG},$$

$$D_{BG} = T\left[\dot{D}_\beta + \dot{D}_\gamma + \dot{D}_{\mathrm{cosm}}\right], \quad (1)$$

where T is the age of the brick, $\dot{D}_\beta$, $\dot{D}_\gamma$ and $\dot{D}_{\mathrm{cosm}}$ the beta-, gamma- and cosmic dose rate, respectively. Specific activities of natural radionuclides in bricks were assessed using low-level

gamma spectrometry. From these values the infinite matrix gamma and beta brick dose rate was calculated using the conversion factors given in Adamiec and Aitken (1998).

The resulting absorbed gamma-dose rate in the measured depth intervals of the bricks is composed of the gamma-dose rate of the brick itself and of the ground/swamp in front of the granary according to:

$$\dot{D}_{\gamma} = f(z) \times \dot{D}^{\infty}_{\gamma,\mathrm{Brick}} + \dot{D}_{\gamma,\mathrm{soil}}, \quad (2)$$

where $f(z)$ is the fraction of the gamma-dose rate in the infinite brick massive observed in brick at depth *z* from the air-brick interface and $\dot{D}_{\gamma,\mathrm{soil}}$ is the absorbed dose rate due to of naturally-occurring gamma-emitting sources in soil at the brick sample location in the wall. Values of the fractional dose rate $f(z)$ for photons emitted by ^{40}K and the radionuclides of the decay series of ^{238}U and ^{232}Th at depth 1 cm were obtained by Monte Carlo simulations (Ulanowski et al., 2019; Woda et al., 2011a).

The contribution of the naturally-occurring radionuclides in soil to the gamma-dose rate of the brick sample was not directly measured in this study. Instead, activity concentrations of the natural radionuclides in soil determined in an earlier study in Muslyumovo, another village located near the banks of the Techa River, 78 km downstream of the release point, were used (Woda et al., 2011a), with conversion factors described in Ulanowski et al., 2019. A relative uncertainty of 50% at the 1-sigma level was assumed, to account for possible differences in radionuclide concentration between Metlino and Muslyumovo. The cosmic dose rate was calculated to be in the range of 0.20–0.23 mGy a^{-1}, depending on sample position, using the methodology described in Woda et al. (2011a), which is based on Prescott and Hutton (1998) and UNSCEAR (2000).

Using the overall error for the cumulative dose σ_{D_L}, the error of the background dose σ_{BG} and the error in the age σ_T, the error of the anthropogenic dose is calculated as:

$$\sigma_{D_X} = \sqrt{\sigma^2_{D_L} + [T\sigma_{\dot{D}_{BG}}]^2 + [\dot{D}_{BG}\sigma_T]^2}\ . \quad (3)$$

3. Results

3.1 Luminescence properties

All samples showed favourable properties in OSL: a strong fast component of the OSL signal, negligible sensitivity changes when applying a 190° preheat and a linear dose response (calibration) curve with low scatter of the datapoints. Obviously in this context, the quartz dosimetric system behaves as if it were in the most simple state of a one trap/ one center model. This gives high confidence in the obtained results. The same applies for TL, for those samples where the

restricted SAR protocol using the 210°C TL peak was applicable and sensitivity changes could be shown to be negligible. Examples of both types of behaviour are illustrated by the upper and lower panel of Fig. 3. Generally, the measurement procedure resulted in homogeneous, narrow dose distributions for the several aliquots measured per sample. Dose recovery tests were conducted on seven depth intervals from different samples, the average ratio of measured to given dose (2 Gy) was 1.00 ± 0.02.

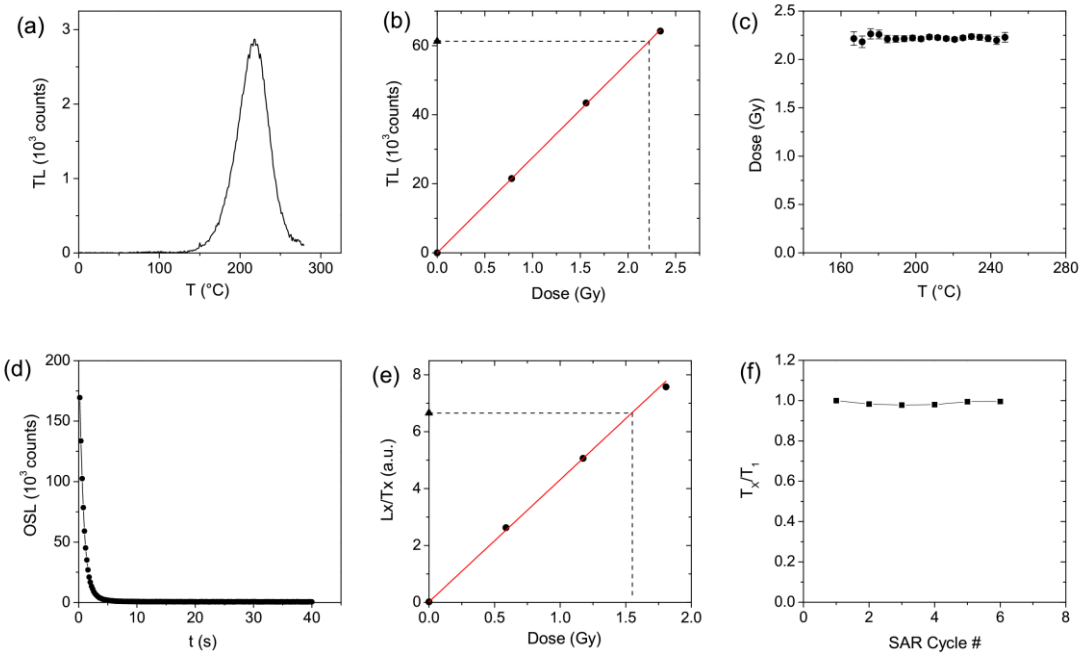

Fig. 2. Upper row: (a) Example TL glow curve, (b) corresponding dose response curve and (c) dose plateau test. Lower row: (d) Example OSL decay curve, (e) corresponding dose response curve and (f) monitoring of sensitivity changes.

3.1.2 Dating of the granary

In Fig. 4 the evolution of measured dose in the different depth intervals for the two samples BG-G1 and BG-G3 is displayed. Whereas for sample BG-G1 no dependency of the measured doses with depth could be observed, a continuous decrease in dose, from around 260 mGy to 208 mGy is seen for sample BG-G3, indicating that only the former was sufficiently shielded and should be used for dating. Measured dose with OSL for BG-G1 is (212±8) mGy and with TL (212±10) mGy, agreeing well within error limits. For the calculation of the dose rate, the gamma-dose rate can be assumed to be entirely composed of the infinite matrix brick gamma-dose rate, as the sample is surrounded by brickwork up to at least 15 cm in all directions. This results in a total dose rate, including beta- and cosmic dose rate of (1.32 ± 0.09) mGy a^{-1}, from which an age of

(161 ± 12) years is calculated. With the year of measurement being 2008, a date of brick production of 1847 [1823-1871] at 95% CI is inferred. There are no other independent age determinations or historical documents to compare the results with but in previous works, the church and mill at Metlino have been dated to 1861 and 1867 [1839-1895] (Degteva et al., 2008). Considering the uncertainty in the ages, the buildings could all be from the same time period, which is a reasonable assumption.

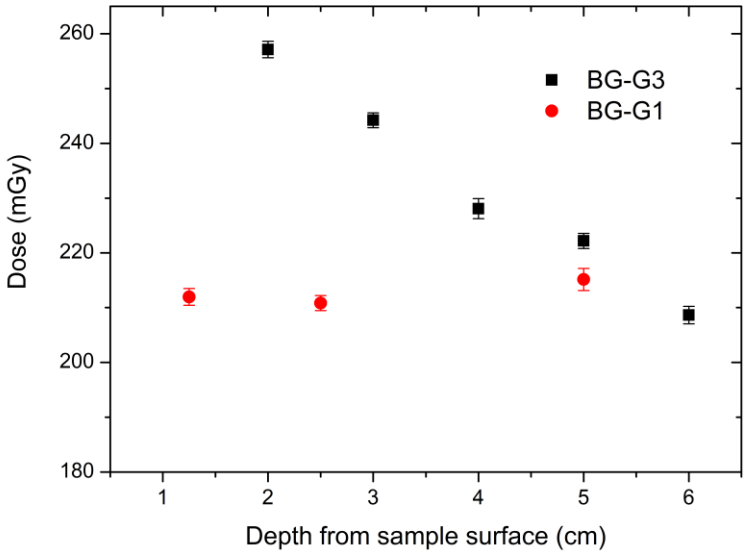

Fig. 4. Dependency of background dose on depth for the two background samples.

3.1.1 Assessment of the background dose rate for the exposed samples

Background dose rates for all exposed samples, calculated from the measured specific activities of natural radionuclides in bricks and considering additional contribution from soil and cosmic particles are listed in Table 1. The brick gamma dose rate amounts to 20-23% of the total dose rate, whereas the gamma dose rate from soil only contributes between 2-6% to the total dose rate. Even though an uncertainty in the soil dose rate of nearly 100% at the two sigma level has to be assumed, the impact on the overall background dose rate is rather small. Similar to previous studies (Woda et al., 2009; Woda et al., 2011a) the dominant contribution stems from the beta dose rate on the quartz grains, which constitutes between 55-68% of the total dose rate. The latter varies in a range typical for bricks, between 2.3 and 2.7 mGy a^{-1} for samples G1/2-G7, whereas for the remaining two brick samples (G13 and G14) the dose rate is about a factor of two lower. Relative uncertainty lies between 4 and 12%, at the one sigma level.

Table 1

Compilation of background dose rate values for samples G1/2–G14. Heights of the sampling points are given above the water level in the Reservoir No. 10. The third column lists the fractional brick gamma-dose rate at 1 cm depth, the fourth column the gamma dose rate of the soil at the sample location and the fifth column the overall gamma dose rate at the sample location.

Sample	height (m)	$\dot{D}_{\gamma,\,\mathrm{B}}$ (mGy a^{-1})	$\dot{D}_{\gamma,\mathrm{S}}$ (mGy a^{-1})	$\dot{D}_{\gamma}$ (mGy a^{-1})	$\dot{D}_{\mathrm{cosm}}$ (mGy a^{-1})	$\dot{D}_{\beta}$ (mGy a^{-1})	$\dot{D}_{\beta+\gamma+\mathrm{cosm}}$ (mGy a^{-1})
G1/2	16	0.45± 0.01	0.05 ± 0.03	0.51± 0.03	0.23 ± 0.05	1.53± 0.26	2.26± 0.27
G3	16	0.63± 0.01	0.05 ± 0.03	0.68± 0.03	0.23 ± 0.05	1.79± 0.09	2.70± 0.11
G4	16	0.52± 0.01	0.05 ± 0.03	0.57± 0.03	0.23 ± 0.05	1.59± 0.14	2.39± 0.15
G5	16	0.54± 0.01	0.05 ± 0.03	0.59± 0.03	0.23 ± 0.05	1.51± 0.06	2.33± 0.08
G6	16	0.50± 0.01	0.05 ± 0.03	0.56± 0.03	0.23 ± 0.05	1.58± 0.18	2.36± 0.18
G7	11.5	0.50± 0.01	0.06 ± 0.03	0.56± 0.04	0.21 ± 0.05	1.52± 0.27	2.29± 0.28
G13	5	0.23± 0.01	0.06 ± 0.03	0.29± 0.03	0.20 ± 0.05	0.68 ± 0.02	1.18± 0.06
G14	5	0.21± 0.01	0.06 ± 0.03	0.28± 0.03	0.20 ± 0.05	0.58 ± 0.02	1.06± 0.06

3.2 Anthropogenic dose and TLD results (granary wall)

Measurement of the cumulative dose was done for all samples using OSL and for samples G1/2, G6, G7 and G14 also using TL (210°C peak). The results are listed in Table 2. Cumulative doses measured in the first cm of the brick range from 0.97 to 2.2 Gy. Dose measurements using OSL and TL agree within error for every brick sample, where both methods could be applied.

individual background doses were calculated from the background dose rate and age of the bricks and are listed in column six of Table 2. After subtraction of the background doses from the cumulative doses, anthropogenic doses in bricks were obtained and range from 0.78 to 1.74 Gy. For samples G1/2, G3 and G4, taken from the same spot, the average anthropogenic dose is 1.73 Gy with a standard deviation of 11 mGy. This variability is smaller than the uncertainty of an individual dose assessment (~ 90 mGy). For samples G13 and G14, at a height of 5 m, the difference in anthropogenic dose is 36 mGy, which is comparable to the estimated measurement uncertainty (32-38 mGy). Both results indicate, that for bricks from this wall, the assessed measurement uncertainty is a realistic measure of the possible variability in doses between brick samples and that this variability is comparatively small. Furthermore, for the bricks from a height of 16 m, the doses assessed for the three samples G1/2, G2 and G3 is statistically not significantly different to the anthropogenic doses for samples G4 and G6, showing that dose deposition along

the granary wall at this height was very homogeneous. One of the reasons for sampling bricks at a relatively large height was that such brick detectors will integrate radiation coming from a large area in front of the wall and should thus be less susceptible to smaller scale variations in the contamination pattern. In contrast, a pronounced dependency of dose on sample height is observed, with doses at 16 m being on average about a factor of two higher than doses at 5 m.

Table 2

Compilation of OSL and TL results for all brick samples from the granary wall in Metlino, for two different depths into the brick. Listed are the cumulative dose (DL), the background dose (DBG) and the anthropogenic dose (DX). Overall errors are quoted at the one sigma level.

Sample	height (m)	Depth (mm)	D_L (mGy)		D_{BG} (mGy)	D_X (mGy)	
			OSL	TL		OSL	TL
G1/2	16	10 ± 5	2094±73	2249±79	364±51	1731±94	1885±95
		20 ± 5	1790±63	1769±62		1426±83	1406±80
G3	16	12 ± 5	2151±75		433±37	1718±91	
		20 ± 5	1913±67			1479±79	
G4	16	10 ± 5	2123±74		384±37	1739±89	
		30 ± 5	1614±57			1230±71	
G5	16	10 ± 5	2070±72		373±31	1697±83	
		30 ± 5	1501±53			1128±62	
G6	16	10 ± 5	2122±74	2205±77	379±41	1743±89	1825±78
		30 ± 5	1530±54	1530±77		1151±69	1151±69
G7	11.5	10 ± 5	1776±62	1741±61	367±52	1408±83	1374±81
		30 ± 5	1506±53	1568±55		1138±75	1200±76
G13	5	10 ± 5	967±34		188±17	779±32	
		30 ± 5	744±26			556±32	
G14	5	10 ± 5	986±34	990±35	170±16	815±38	819±43
		30 ± 5	705±25	649±23		534±30	479±31

The dose depth profile for samples G1-2, G7 and G14 is shown in Figure 5. A similar exponential decrease of the relative dose with depth is seen, irrespective of the sample height. Using the additional doses at the depths of 2 and 3 cm for the other samples in Table 2, an average D_{X-20}/D_{X-10} and D_{X-30}/D_{X-10} ratio of 0.83 ± 0.03 and 0.68±0.03 is calculated, respectively. Within uncertainty, these values are in general agreement with an attenuation calculated for gamma-rays with energies larger than 600 keV that were emitted by radionuclides on the ground in front of a wall (ICRU, 2002).

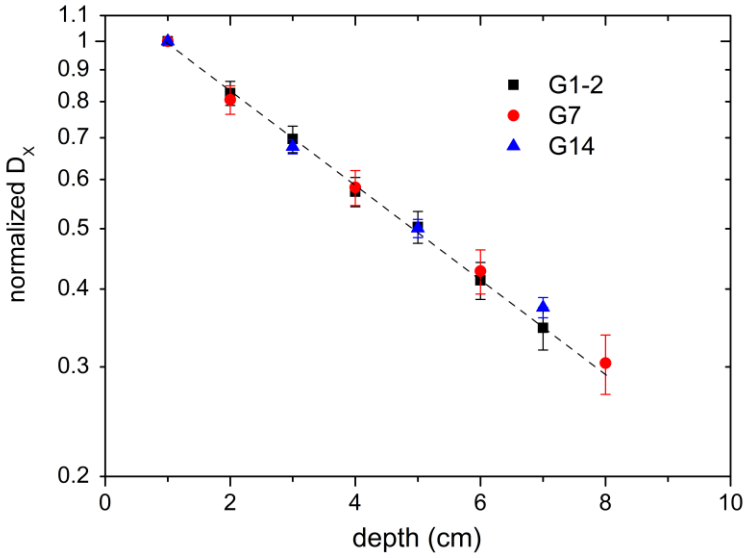

Fig. 5. Measured dose-depth profile for selected samples.

The results of the assessment of the contemporary gamma dose rate at the brick sample positions, as measured by the TLDs, is given in Table 3. Dose rate in TLD varies from 10.4 mGy a^{-1} for the topmost samples to 4.53 mGy a^{-1} for the lowermost samples, showing almost exactly the same dependence on height as the values for the anthropogenic doses in bricks do. Dose rates measured with the Automess dose rate meter during sampling are in a similar range of values as the TLD results, although it should be kept in mind that the former is measuring dose in air in front of the bricks, the latter the dose in (shielded) TLD 1 cm into the brick. Using conversion factors *CF* of 0.6 to 0.65 (±0.06), depending on sample height, the dose rate in TLD can be converted to dose rate in brick at the same depth of 1 cm (e.g. dose rate for the quartz grains within the brick) (Ulanowski et al., 2019). Since the variation in dose conversion coefficients is less than 10%, the same height profile is also observed for the dose-rate in brick, with the values decreasing from 17.3 mGy a^{-1} for the topmost sample to 6.97 mGy a^{-1} for the lowermost sample.

Table 3

Gamma dose-rate in TLD, stored for one year at 1 cm depth in bricks adjacent to brick samples G4, G7 and G13. The given values are the average and standard devation of the results of three TLDs per sample. Also listed is the dose-rate in air (3rd column), measured at the sample position using an Automess AD18 dose-rate meter and the dose-rate in brick (5th column), calculated from the dose-rate in TLD. Overall errors are quoted at the one sigma level.

Sample	height (m)	$\dot{D}_{air}$ -Automess (mGy a^{-1})	$\dot{D}_{TLD}$ (mGy a^{-1})	$\dot{D}_{brick}$ (mGy a^{-1})
G4	16	8.8 – 13.1	10.38 ± 0.37	17.30 ± 1.84
G7	11.5	8.6 – 10.5	8.65 ± 1.04	13.96 ± 2.16
G13	5	4.3 – 5.3	4.53 ± 0.14	6.97 ± 0.68

3.3 Field mapping and TLD results (above soil)

The results of the dose rate measurements in air in the area in front of the granary is shown in Fig. 6. The dryland close to the dam and the languet extending into the swampy area are contaminated on a comparatively low level, with dose rates ranging from 2.5 -5 µGy h^{-1}. In contrast, the accessible swampy area to the north and northwest of the granary, together with a small strip at the border swamp/dryland shows a factor of 5-10 higher dose-rates (13-45 µGy h^{-1}). The measurements are in general agreement with the dose rates in air derived from TLDs (Table 4), which have accumulated dose for over two months, indicating that the field mapping results, which are a snapshot of one or two days during the sampling campaign, can be regarded as representative for the months without snow cover. The area extending from the dam directly to the granary wall was not systematically mapped but from selected point measurements, it can be concluded that the overall contamination level is lower than for the lowest contaminated area on the other side of the damn (1-2 µGy h^{-1}).

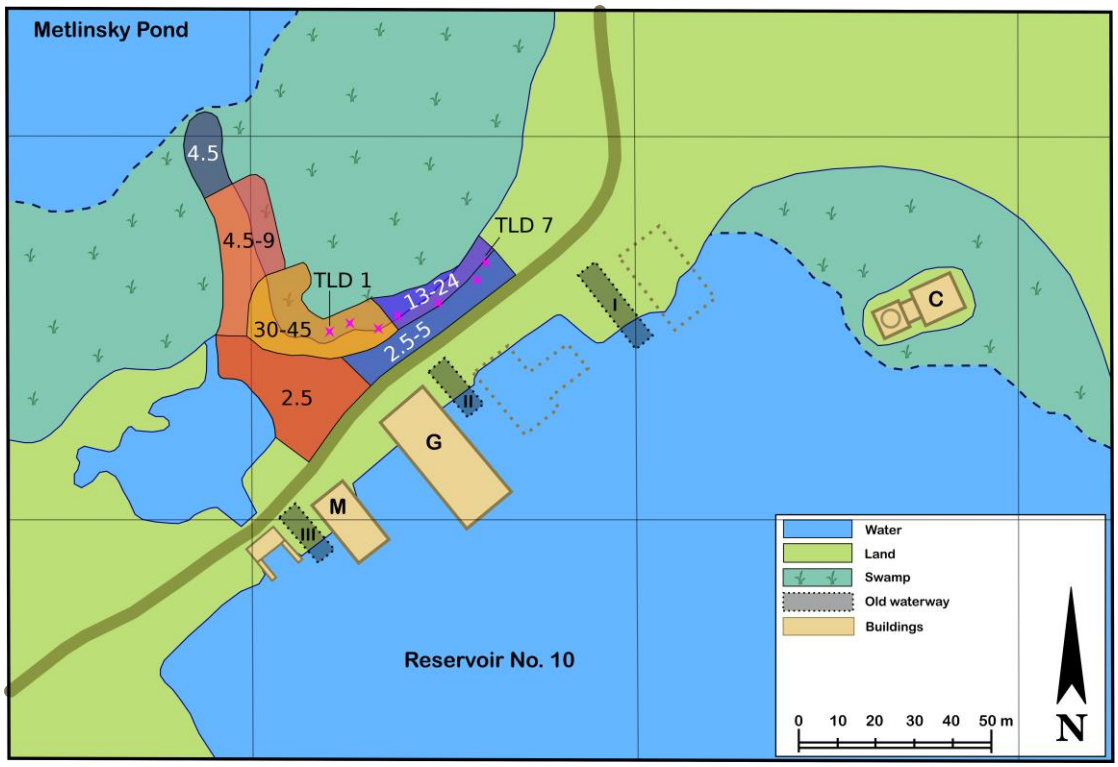

Fig. 6. Results of the dose-rate mapping in units of µGy h^{-1}. TLD positions are indicated by stars.

Table 4

Dose-rate in air, 1 m above ground, measured by TLDs. Per position, the average and standard deviation of the results of four dosimeters is given. The last column lists the dose-rate measured near the TLD position using the dose-rate meter during sampling in September 2012.

TLD Position #	$\dot{D}$ (µGy h^{-1})	$\dot{D}$ –Automess (µGy h^{-1})
1	25.6 ± 1.2	28.1
2	31.6 ± 0.1	28.4
3	29.6 ± 0.5	31.7
4	23.0 ± 0.6	24.8
5	26.9 ± 0.2	33.0
6	20.3 ± 0.7	13.5
7	22.8 ± 0.6	24.4

4. Discussion

The increase of the present-day gamma dose-rate in bricks with height above ground, as measured by TLDs, might appear at first surprising, since it could be intuitively expected that dose rates drop with increasing distance from the sources. Indeed, it has been shown in previous exemplary Monte Carlo calculations, that for gamma rays of 662 keV energy and emitted from radionuclides homogeneously deposited on an area starting from immediately in front of a brick wall and up to a distance of 200 m, a decrease in dose is calculated with increasing sample height, contrary to what is observed here (ICRU, 2002). However, if radionuclides are deposited on an area between 35 and 100 m distance to the wall (i.e. no more close sources) a slight increase of anthropogenic doses is calculated for an increasing sample height (ICRU, 2002). This is qualitatively similar to the source geometry of the present study site, with the highest contaminated areas and dominating sources located at a distance of more than 20 m from the granary wall, whereas the closer located areas show almost an order of magnitude lower contamination levels. Although the dose rates in the entire swampy area north-east and also north-west of the granary wall could not be mapped, it is likely that similar dose-rates to the ones measured at the beginning of the swamps would be measured, meaning that the sources of major exposure of the bricks may be more extended than Fig. 6 indicates. Additionally it has to be taken into account, that radionuclides are not only present on the soil surface but have migrated into soil up to at least 30 cm depth (Hiller et al., 2017). This is expected to result in lower attenuation for gamma-rays reaching the higher located samples, increasing the dose-height profile. Indeed, a 50% increase in dose for samples from 4 to 12 m heights has been measured for bricks from the mill in Muslyumovo, where a similar source geometry with depth distribution in ^{137}Cs activity is encountered (Woda et al., 2011a). Also for the west-southwest wall of the church tower in Metlino and the (historic) source geometry, reconstructed for the time period 1949-1956, an increase in dose at 19.6 m height of 34% compared to the dose at 3.6 m height was calculated by Monte-Carlo simulations (see Fig. 15 and Table 5 in Hiller et al. (2017)). The higher dose ratio of a factor of two observed for the north-western granary wall in this study could either be caused by additional attenuation effects due to the higher water content of the swamp or by possible shielding effects of the lowermost sample at 5 m height due to the (reinforced) damn. Ultimately, only radiation transport calculations will enable a full comparison of assumed source geometry and observed dose height profile, which is the focus of the follow-up, full-scale validation study of the TRDS-2016, mentioned in the introduction.

It is remarkable that the anthropogenic doses in the bricks, as illustrated in Fig. 7, show almost the same height profile as the present-day gamma dose-rate in bricks. However, caution must be exercised when interpreting this agreement. Doses in TLDs have been integrated over one year and are directly correlated to the present-day contamination pattern. Anthropogenic doses in bricks have accumulated over fifty years, where it is known from historic documents that that exposure geometry changed significantly (Degteva et al., 2016; Mokrov, 2002). Highest contamination levels and thus exposure rates above the water surface of the Metlinsky pond and at its shoreline occurred in the second half of 1951, whereas in the following year measures were

undertaken that decreased the dose-rate by two orders of magnitude: construction of new or rebuilding and extension of existing earth dams to both sides of the Metlinsky pond facing the Metlino village and rebuilding (increasing) of the damn in front of the granary (called damn D-4). Uncontaminated soil was used for this purpose. After finishing the constructions, the water level of the pond was raised by one meter, covering and shielding the most contaminated sites at the shoreline. In addition, as illustrated in Fig. 1, new sources (the swampy areas) were created over time after 1952 by accumulation of radioactive sediment near dam D-4. The origin of these deposits is likely the upper part of the pond with an increased specific activity. These different contributions to the brick doses have to be carefully reconstructed/assessed using available historic information on contamination levels and radiation transport calculations. At this stage, it cannot be decided whether the similarity of the dose and present dose rate profile for the brick wall is an indication that the current source geometry can be seen as representative for the relevant time period of accumulation of anthropogenic dose in bricks or whether the similarity is by chance.

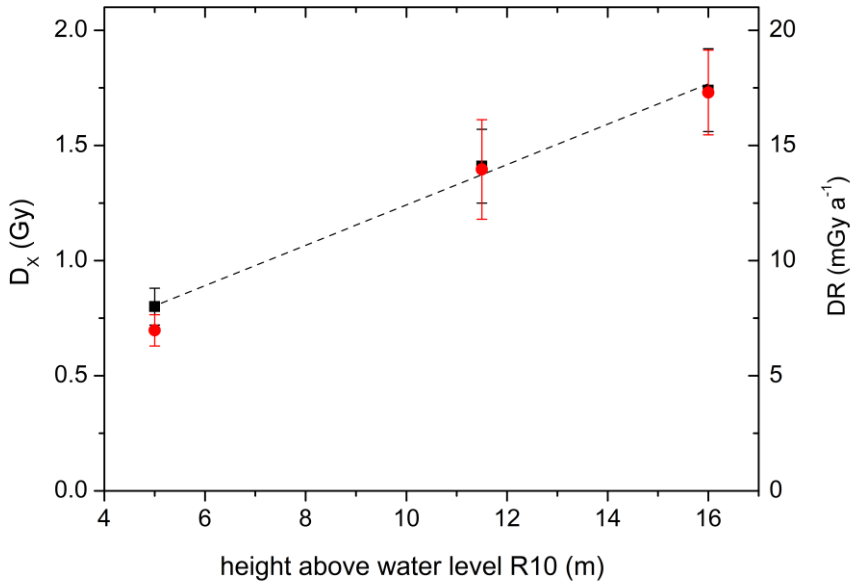

Fig. 7. Dependency of anthropogenic doses in bricks (black square symbols) and dose-rate in bricks, derived from TLDs (red circle symbols), on sample height. The dashed line is a linear fit to the DX measurements for the purpose of illustration of the continuous increase with height.

It has already been described in section 3, that the attenuation of dose in brick up to a depth of 2 to 3 cm is compatible with an assumption that radionuclides, emitting photons with energy greater than 600 keV, are homogeneously distributed on the ground in front of a wall. On the other hand it has been further shown in Woda et al. (2011a), based on the calculations presented in ICRU (2002) and Göksu et al. (2002), that similar (simulated) dose-depth profiles are

obtained for ^{137}Cs distributed in soil up to a depth of 6 g cm^{-2} and for radionuclides distributed on the ground only and emitting photons at 334 keV. This is due to the higher contribution of scattered photons in the case of radionuclides distributed in soil, having lower photon energies than the unscattered radiation and thus experiencing stronger attenuation with depth into brick. A more meaningful comparison of the measured dose-depth profile shown in Fig. 5 with modelled data thus requires in-depth radiation transport calculations for the assumed source configuration and energy, which is the scope of the follow-up study. Nevertheless, already at the present stage it seems that the dose-depth profile may be used to confirm the source energy but may not be sensitive enough to allow discrimination between different possible combinations of source energy and source configuration.

5. Summary and Conclusions

Several bricks from the north-western wall of the granary in Metlino, facing the Metlinsky Pond, were sampled and the anthropogenic doses measured for the purpose of dose reconstruction. All samples, except for sample G9, showed excellent dosimetric properties in TL and OSL, giving confidence in the obtained results. The measured gamma dose rate height profile (from TLDs in the wall) seems on a qualitative level to be compatible with the current source geometry, assessed from dose rate and TLD measurements above soil on a larger area in front of the granary. The current gamma dose rate height profile is very similar to the dose-height profile measured in bricks, however, this is not readily interpretable due to the complex changes in the exposure geometry that occurred since the beginning of the contamination in the early 1950s until today. In this context, the measured doses, dose rates, dose-height and dose-depth profiles can give valuable experimental constraints to limit the number of possible source configurations and energies. It will be seen in the full scale validation study to follow, how this can be combined with available historic information on contamination patterns, levels and exposure rates to derive the integral air kerma at the shoreline of the Metlinsky Pond from 1949-1956 and in this way to further validate the TRDS-2016.

Acknowledgements

The research leading to these results has received funding from the European Community's Sixth Framework Program (FP6-516478) and Seventh Framework Program (FP7/2007-2013), the latter under grant agreement n°249675. Financial support to fully analyse and publish these data was provided by the Russian Health Studies Program of the U.S. Department of Energy (DOE) under the auspices of the Joint Coordinating Committee for Radiation Effects Research Project 1.1, Techa River Population Dosimetry. We are grateful to administration of the Mayak Production Association for providing personnel and the truck with hoisting platform for sampling the granary wall and to Dr. Y. Mokrov for valuable information on the history of the studied site.

References

Adamiec, G., Aitken, M., 1998. Dose-rate conversion factors: update. Ancient TL 16, 37-50.

Aitken, M., 1985. Thermoluminescence dating. Academic Press Inc., London.

Bailiff, I.K., Bøtter-Jensen, L., Correcher, V., Delgado, A., Göksu, H.Y., Jungner, H., Petrov, S.A., 2000. Absorbed dose evaluations in retrospective dosimetry: methodological developments using quartz. Radiat. Meas. 32, 609-613.

Bailiff, I.K., Petrov, S.A., 1999. The Use of the 210°C TL Peak in Quartz for Retrospective Dosimetry. Radiat. Prot. Dosim. 84, 551-554.

Bailiff, I.K., Stepanenko, V.F., Göksu, H.Y., Bøtter-Jensen, L., Brodski, L., Chumak, V., Correcher, V., Delgado, A., Golikov, V., Jungner, H., Khamidova, L.G., Kolizshenkov, T.V., Likhtarev, I., Meckbach, R., Petrov, S.A., Sholom, S., 2004a. Comparison of retrospective luminescence dosimetry with computational modeling in two highly contaminated settlements downwind of the Chernobyl NPP. Health Phys. 86, 25-41.

Bailiff, I.K., Stepanenko, V.F., Göksu, H.Y., Jungner, H., Balmukhanov, S.B., Balmukhanov, T.S., Khamidova, L.G., Kisilev, V.I., Kolyado, I.B., Kolizshenkov, T.V., Shoikhet, Y.N., Tsyb, A.F., 2004b. The application of retrospective luminescence dosimetry in areas affected by fallout from the Semipalatinsk Nuclear Test Site: an evaluation of potential. Health Phys. 87, 625-641.

Degteva, M.O., Bougrov, N.G., Vorobiova, M.I., Jacob, P., Yeter Goksu, H., 2008. Evaluation of anthropogenic dose distribution amongst building walls at the Metlino area of the upper Techa River region. Radiat. Environ. Biophys. 47, 469-479.

Degteva, M.O., Shagina, N.B., Vorobiova, M.I., Shishkina, E.A., Tolstykh, E.I., Akleyev, A.V., 2016. Contemporary understanding of Radioactive Contamination of the Techa River in 1949-1956. Radiat. Biol. Radioecol. 56, 523-534 (in Russian).

Galbraith, R., 2002. A note on the variance of a background-corrected OSL count. Ancient TL 20, 49-51.

Goksu, H.Y., Bailiff, I.K., 2006. Luminescence dosimetry using building materials and personal objects. Radiat. Prot. Dosim. 119, 413-420.

Göksu, H.Y., Degteva, M.O., Bougrov, N.G., Meckbach, R., Haskell, E.H., Bailiff, I.K., Bøtter-Jensen, L., Jungner, H., Jacob, P., 2002. First international intercomparison of luminescence techniques using samples from the Techa River valley. Health Phys. 82, 94-101.

Hiller, M.M., Woda, C., Bougrov, N.G., Degteva, M.O., Ivanov, O., Ulanovsky, A., Romanov, S., 2017. External dose reconstruction for the former village of Metlino (Techa River, Russia) based on environmental surveys, luminescence measurements, and radiation transport modelling. Radiat. Environ. Biophys. 56, 139-159.

ICRU, 2002. Retrospective Assessment of Exposures to Ionising Radiation.

Jacob, P., Goksu, Y., Taranenko, V., Meckbach, R., Bougrov, N.G., Degteva, M.O., Vorobiova, M.I., 2003. On an evaluation of external dose values in the Techa River Dosimetry System (TRDS) 2000. Radiat. Environ. Biophys. 42, 169-174.

Meckbach, R., Bailiff, I.K., Göksu, Y., Jacob, P., Stoneham, D., 1996. Calculation and Measurement of Depth Dose Distributions in Bricks. Radiat. Prot. Dosim. 66, 183-186.

Mokrov, Y.G., 2002. Reconstruction and prediction of radioactive contamination of the Techa River (Parts I and II). Publishing Center of Radiation Safety Problems, Ozersk (in Russian).

Mokrov Y.G., Stukalov, PM, Martyushov, VZ., 2005. To the problem of external exposure dose estimation for Metlino residents (the Techa River, Chelyabinsk region) in the early 1950s. Radiat Safety Problems (Mayak Production Association Scientific Journal) № 4:51-57; 2005 (in Russian).

Murray, A.S., Wintle, A.G., 2003. The single aliquot regenerative dose protocol: potential for improvements in reliability. Radiat. Meas. 37, 377-381.

Prescott, J.R., Hutton, J.T., 1988. Cosmic ray and gamma ray dosimetry for TL and ESR. International Journal of Radiation Applications and Instrumentation. Part D. Nuclear Tracks and Radiation Measurements 14, 223-227.

Prescott, J.R., Hutton, J.T., 1994. Cosmic ray contributions to dose rates for luminescence and ESR dating: Large depths and long-term time variations. Radiat. Meas. 23, 497-500.

Taranenko, V., Meckbach, R., Degteva, M.O., Bougrov, N.G., Goksu, Y., Vorobiova, M.I., Jacob, P., 2003. Verification of external exposure assessment for the upper Techa riverside by luminescence measurements and Monte Carlo photon transport modeling. Radiat. Environ. Biophys. 42, 17-26.

Ulanowski, A., Hiller, M.M., Woda, C., 2019. Absorbed doses in bricks and TL-dosimeters due to environmental radiation sources, submitted.

UNSCEAR, 2000. Sources and effects of ionizing radiation. Annex B: Exposures from natural radiation sources.

Werner, C.J. (editor), 2017. MCNP Users Manual - Code Version 6.2. LA-UR-17-29981.

Wintle, A.G., Murray, A.S., 2006. A review of quartz optically stimulated luminescence characteristics and their relevance in single-aliquot regeneration dating protocols. Radiat. Meas. 41, 369-391.

Woda, C., Jacob, P., Ulanovsky, A., Fiedler, I., Mokrov, Y., Rovny, S., 2009. Evaluation of external exposures of the population of Ozyorsk, Russia, with luminescence measurements of bricks. Radiat. Environ. Biophys. 48, 405-417.

Woda, C., Ulanovsky, A., Bougrov, N.G., Fiedler, I., Degteva, M.O., Jacob, P., 2011a. Luminescence dosimetry in a contaminated settlement of the Techa River valley, Southern Urals, Russia. Radiat. Meas. 46, 277-285.

Woda, C., Ulanovsky, A., Bougrov, N.G., Fiedler, I., Degteva, M.O., Jacob, P., 2011b. Potential and limitations of the 210°C TL peak in quartz for retrospective dosimetry. Radiat. Meas. 46, 485-493.